ACS OMEGA

Open Access



http://pubs.acs.org/journal/acsodf

Article

# Fluorophore-Induced Plasmonic Current Generation from Copper Nanoparticle Films

*Published as part of the ACS Omega virtual special issue "Celebrating 50 Years of Surface Enhanced Spectroscopy".*

Daniel R. Pierce, Lahari Saha, and Chris D. Geddes*

Cite This: *ACS Omega* 2024, 9, 25181−25188

Read Online

ACCESS | Metrics & More | Article Recommendations | Supporting Information

**ABSTRACT:** We describe the process of generating a fluorophore-induced plasmonic current (FIPC) from copper nanoparticle films. Previous work and the literature have shown that excited near-field fluorophores are able to plasmonically couple with metal nanoparticle films (MNFs), inducing surface plasmons in the films. These induced surface plasmons are then in turn able to generate a directly measurable electrical current across the film. These generated currents have been quantified and detected in noble metal films, such as those made from Ag and Au, but due to the cost of such films, there has been a push to use lower cost materials for FIPC. Previous work has detailed the use of gold, silver, and aluminum films for these purposes, and in this paper, we will subsequently examine the ability of thermally deposited copper films to generate FIPC when in close proximity to excited near-field fluorophores. We report the effects of copper film thickness, the effects of light polarization and solution conductance, and the effects of metal-enhanced fluorescence (MEF) emission on the generation of plasmonic current.

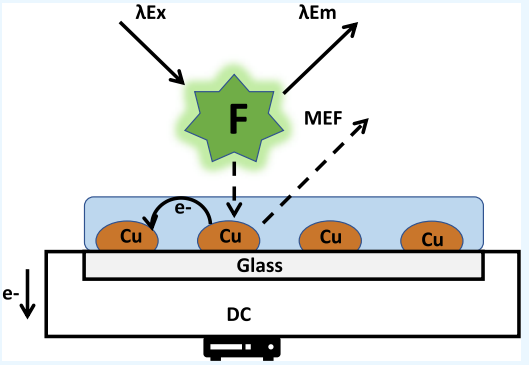


## 1. INTRODUCTION

Literature on the phenomenon known as metal-enhanced fluorescence (MEF)[1−14] has detailed that when a fluorophore is in close proximity to a metal nanoparticle, under the appropriate conditions, the fluorophore may couple to the plasmonic particle, which ultimately leads to an enhanced fluorescence intensity, by way of altering the free space properties of the fluorophore and increasing the rate of emission from the coupled system. These free space property changes are believed to be due to the ability of the nanoparticle to function as a microantenna and allow the nanoparticle−fluorophore complex to absorb more light than the uncoupled fluorophore alone. This enhancement, coupled with a much faster and more energetically favorable route of emission, leads to an increase in the fluorescence intensity of the fluorophore and a decrease in the emission lifetime. This effect is only observed when the spectral overlap (absorption and emission) between the fluorophore and the film nanoparticles is notable.[2−6] Recent work by our group has shown that under certain conditions, this coupling event is able to generate a novel phenomenon known as fluorophore-induced plasmonic current (FIPC), wherein instead of an enhanced fluorescence emission from the complex, a detectable current is now also observed across the nanoparticle film, upon the excitation of the fluorophore−nanoparticle complex.[15−18,24] This generated current has been experimentally linked to MEF emission, wherein MEF emission decreases as the magnitude of current generation increases, demonstrating a conservation of energy within the system.

This current generation is believed to be due to nonradiative energy transfer from the excited-state fluorophore to an individual nanoparticle on the film. The individual nanoparticle absorbs energy until its capacitance is reached, after which time it will discharge its energy.[15] If a nanoparticle of the appropriate size and conductivity is nearby, the energy can be transferred from particle to particle in a process known as electron hopping, described in the previous literature by our group.[15−18,24] This hopping electrical charge across the surface of the film can be detected as current when measured across the entire film. It has been experimentally shown that there are several factors that impact the magnitude of the detectable current: the molar extinction coefficient of the fluorophore; the concentration of the fluorophore; the position of the excitation

Received: March 21, 2024
Revised: May 2, 2024
Accepted: May 9, 2024
Published: May 24, 2024

irradiance relative to the electrodes placed on the film; the power and polarization of the excitation incident light exciting the system, and the temperature of the system.[15−18]

In this paper, we have subsequently investigated the FIPC from a range of different density thermally deposited copper nanoparticle films. Copper is a widely available inexpensive metal that provides a method for making FIPC detection more affordable than the use of noble metals such as gold and silver. While FIPC has been shown to be generated from aluminum nanoparticle films,[24] it should be noted that these films are only useful with UV-absorbing fluorophores and are also less chemically and physically stable. Copper, however, is plasmonically active in different wavelength ranges compared to previously studied film types made of gold, silver, and aluminum and can be useful for fluorophores that would not normally have a strong spectral overlap with the previously studied metals.

## 2. MATERIALS AND METHODS

The copper MNFs that were used in this study were produced in our laboratory through the use of thermal vapor deposition, a process which is described in previous publications from our laboratory.[19,20,24] Silane-coated glass slides are first washed and dried with ethanol and then attached to the rotary stage of an Edwards auto-306 thermal vapor deposition unit, with the silane-coated glass side directly above the metal sublimation area. Under a vacuum strength of $2 \times 10^{-5}$ Torr, the copper metal is sublimated through the application of a high current, heating the copper in a molybdenum boat, leading to gaseous Cu. The desired deposition rate of the metal is achieved through the regulation of the applied current (extent of heating), and the rate used here was between 0.1 and 0.2 Å/s. For these copper films, a final thickness of 1.5, 2, 2.5, 3, and 3.5 nm was obtained, and once produced, they were stored in a vacuum desiccator until use. The thickness is determined via deposition on a crystalline sensor directly next to the sample deposition area and is such an approximation of the deposition on the film. The absorbance characteristics of these films are detailed in Figure 1, and as shown, as the amount of deposited copper increases, the absorbance in both the UV/blue spectral region (350−475 nm) and red region (700−800) subsequently increases. This increase in absorption in these regions is due to the spectral properties of the nanoparticles changing as they grow in size from isolated particles and eventually into each other to form a continuous metal film.[16,24] Previous work by

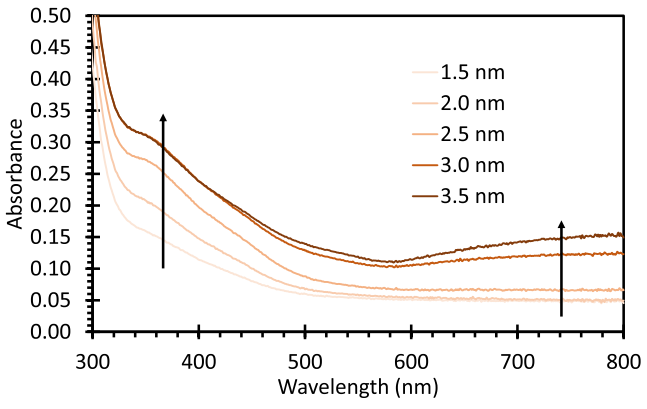


**Figure 1.** Absorbance spectra of thermally deposited copper films; the overall absorbance increases with the increasing thickness of the film.

our group has shown that noncontinuous particulate metal films are the optimal choice for generating plasmonic current, and these can be characterized by simply determining the resistivity of the films through the application of a current across their surface. Through a technique known as voltage sweeping, described previously,[15] we are able to determine the overall resistivity of the films as well as their ability to charge and discharge energy through different-sized particles. This process of charging and discharging energy ultimately leads to a "staircase-like effect" on a chart plotting applied voltage against observed current and is due to a well-known phenomenon known as a coulombic blockade.[15] However, this effect is not seen in the continuous metal films. For this reason, semicontinuous films are ideal for FIPC generation, and for copper nanoparticle films, the ideal thickness was found to lie between 1.5 and 3.5 nm.

FIPC experiments were performed in accordance with our group's methodology,[15−18,24] with the experimental setup shown in Figure 2. In short, the film is placed onto a

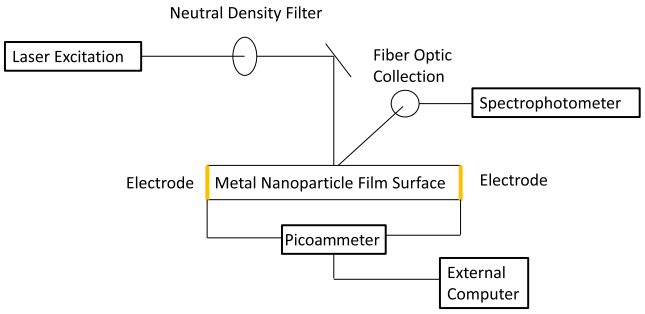


**Figure 2.** Experimental collection of plasmonic current. Excitation light from a CW laser is passed through a neutral density filter before falling incident on the sample stage, exciting the fluorophore on the surface of the film. Fluorophore-induced plasmonic current is collected through electrodes in series with a picoammeter, and the fluorescence emission for MEF is collected via a fiber optic cable.

nonelectrically conductive sample stage and is connected in series to a Keithley 6487 picoammeter through the use of copper electrodes. The film is then tested dry, with deionized water, and then with a fluorophore, the fluorophore being the one selected that has a strong spectral overlap with the absorptive characteristics of the copper film.[15−18,24] For this experiment, we used varying concentrations of fluorescein disodium salt, from 5 to 100 $\mu$M. These solutions were excited with a 473 nm solid-state laser (Quvl473-20 Laser Mate), with a constant power of 10 mW, through the use of a neutral density filter. The experimental data are shown in Figure 3, where the background current of the system is initially captured, the laser is exposed to the sample for 1 s, and then, the laser is gated such that the exposure to light stops. The change in current, its modulus, both before and after exposure is tabulated and reported for each individual data point. This is known as the absolute current as opposed to the direct current readout from the system. For these experiments, the data shown are the average of several of these individual gated excitations. The significant increase in current in the presence of a fluorophore can readily be seen by noting the magnitude of the current ($y$-axis), i.e., by comparing the three panels of Figure 3.

Experiments studying the differences in fluorescence intensity between MEF and FIPC conditions were performed


https://doi.org/10.1021/acsomega.4c02751
ACS Omega 2024, 9, 25181−25188

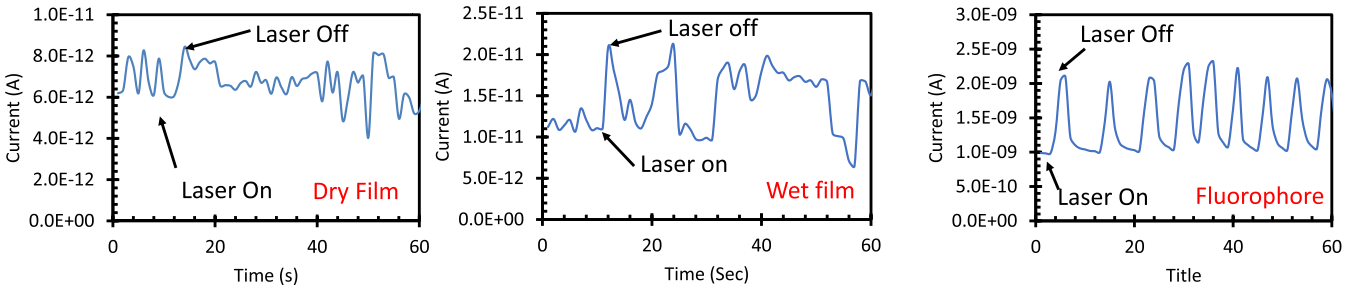


**Figure 3.** Current response to 473 nm laser excitation: Dry film (left), wet film with $H_2O$ (middle), and film with 50 $\mu$M fluorescein (right). The words on the figures "Laser On" and "Laser Off" represent the on and off states for the excitation of the film, respectively, and its solutions, while in series with the current detection device. Laser excitation was pulsed for 1 s, and the laser on and off timing is noted for the initial exposure. The difference before and after the exposure is recorded, and the FIPC values are derived from the difference between the two states.

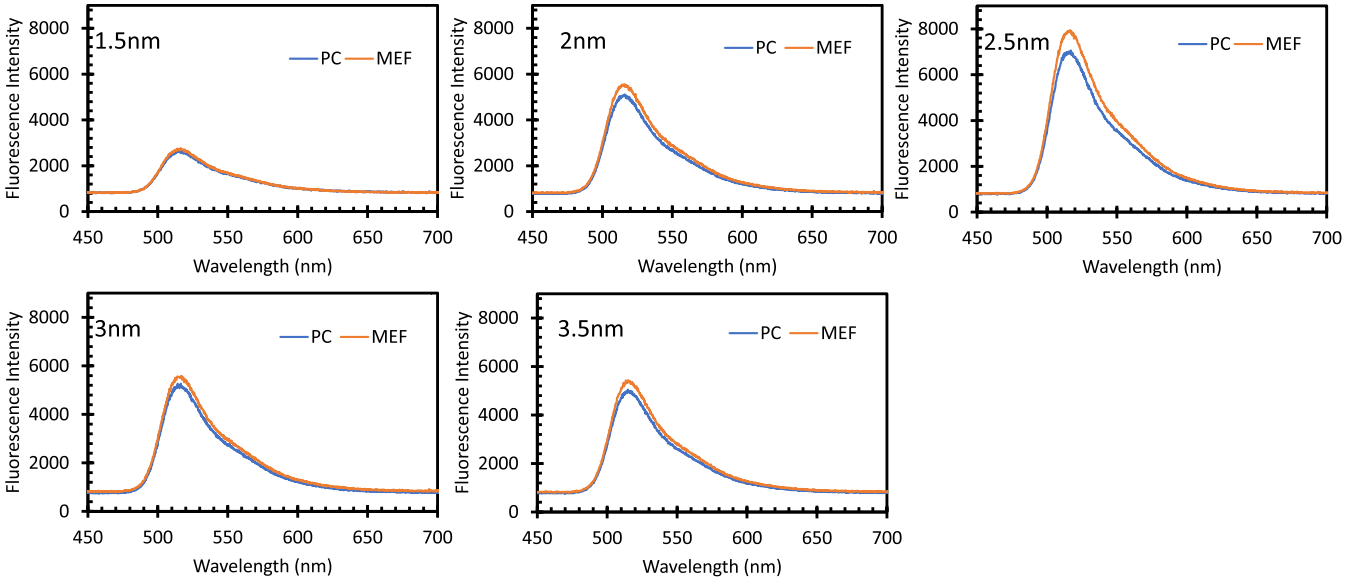


**Figure 4.** Fluorescence intensity vs wavelength plots for 5 $\mu$M fluorescein excited via a 473 nm laser on 1.5 → 3.5 nm Cu films under conditions supporting both metal-enhanced fluorescence (MEF) and fluorophore-induced plasmonic current (FIPC). Conditions for MEF generation being where the fluorophore is directly on the surface of film and for PC being the same with an additionally attached picoammeter, with a bias current (0.005 V) applied.

in the same manner as a typical FIPC experiment, while now subsequently collecting emission through a fiber optic cable spectrophotometer (ocean optics). The fluorescein solutions were excited in experimental setups both with and without an applied bias current, to simulate both FIPC and MEF, respectively, and to compare between the two, similar to prior work.[15,16,24] The use of a bias current has been described by our group as a method to dictate and assign the anode and cathode, ultimately reducing run-to-run variability. For each of these experiments, the emissions from each condition are tabulated and reported in Table 2 and shown graphically in Figure 4.

## 3. RESULTS AND DISCUSSION

**3.1. Effect of Film Thickness on the Photophysical and Electrical Properties of Cu Films.** It is well known that the photophysical and optical properties of a plasmonic film change as the thickness of the film increases.[15−19] This is due to the spectral and electrical properties of the individual nanoparticles changing as they grow in size, change shape, and close the interparticle distance between discrete nanoparticles.[15−18,24] For this analysis, we studied five different thicknesses of copper films, ranging from 1.5 to 3.5 nm in half nm thickness increments, and subsequently characterized them with regard to their ability to generate current. Figure 1 details the absorbance of the films of thickness 1.5−3.5 nm, and Supporting Figure S1 details thicknesses ranging from 1 to 15 nm; however, these films were not all characterized for FIPC as many of them were found to be unviable, i.e., too thick. From Figure 1, we can see that there are two major regions where increased thickness leads to an increased absorbance: in the UV spectral range from 300 to 500 nm and in the red wavelength range from 700 to 700 nm and beyond with the largest absorbances seen in the 3.5 nm films as expected. This is to be expected as the increased density of nanoparticles leads to an increased absorption of light relative to the silane glass slide substrate support.[21,24] In Supporting Figure S1, we can see that as film thickness increases, we start to see a dramatic increase in the absorption of the thicker films (10 → 15 nm) in the regions above 600 nm, eventually losing the copper nanoparticle plasmon band and instead displaying mirror-like properties indicative of a solid metal continuous film. These thicker films were found to be continuous and not suitable for FIPC experiments due to a high background current, a reduced film resistance, and little interaction with the fluorophore upon


https://doi.org/10.1021/acsomega.4c02751
ACS Omega 2024, 9, 25181−25188

excitation. The films shown in Figure 1 were subsequently characterized through a series of voltage sweep experiments.[15,16,24] The films were placed onto the FIPC testing stage (Figure 2) and the copper electrodes were attached. Over a 10 s period, a voltage was applied, starting at 1 V and then progressing slowly to 10 V, at a rate of 1 V per second. For a solid sheet of continuous metal or other comparable conductor, there would be a linear relationship between **V** and **I**, such that as the voltage increases, the current should accordingly be as the resistance is fixed for these films. For our films, we have observed that for noncontinuous nanoparticle films, a coulombic blockade is seen, and the charge and discharge cycle of the discrete nanoparticle modulation results in a current response that modulates, irrespective of the applied voltage (Figure 5). We see this modulation for all of

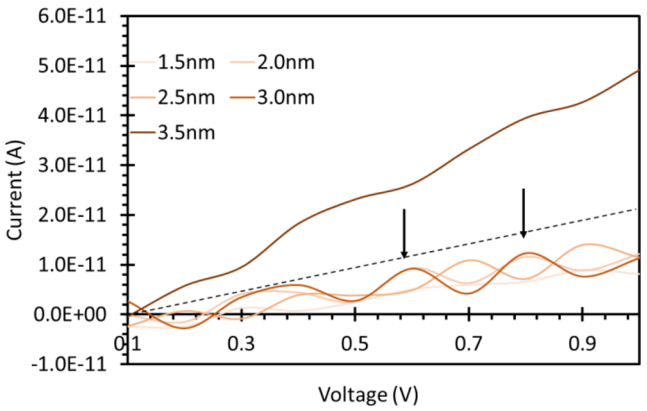


**Figure 5.** Voltage vs current sweep experiments (coulombic staircase), for increasing voltages applied to 1.5−3.5 nm-thick thermally evaporated copper films. A control line has been added to represent a linear relationship between voltage and current with a fixed resistance (dotted black line).

the films tested; however, it should be noted that for the 3.5 nm films, the response is more in line with a continuous film, as we see more of the linear relationship between **V** and **I**. Films not included in this study were ones that displayed the linear relationship between **V** and **I**; however, a control dataset has been included for comparison. For copper films, it was found that for 4 nm and thicker, this was observed, and we subsequently deemed them not appropriate for FIPC experiments.

The capacitance of the stairs in the coulombic staircase can be derived from the following equation

$$C_{\text{gate}} = \frac{\Delta U}{\Delta Q} \tag{1}$$

where $\Delta Q$ is the charge needed to induce one oscillation in the staircase pattern, $\Delta U$ is the electrical charge in coulomb, and $C$ is the capacitance of the film. The calculated values that are shown in Table 1 are derived from applying this formula to the first and second staircases seen in Figure 5 (arbitrarily chosen). The concentric sphere model for nanoparticle capacitance (eq 2)[15] suggests that as the sizes of the particles increase, the capacitance of the film will also increase, and this is seen across all five tested films as the film thickness increases. Previous reporting from our group has used this model when determining the capacitance of a discrete nanoparticle.[15,16]

$$C = 4\pi\varepsilon_0\varepsilon r_0(r_0 + s)/s \tag{2}$$

**Table 1. Calculated Capacitance of the Films from the Staircase in Figure 5, Determined from the Difference in Current at the Peaks of Each Coulombic Staircase Maxima (Shown by Arrows), Divided by the Change in Voltage over that Range**

| film thickness (nm) | calculated capacitance (F) |
|---|---|
| 1.5 | $1.26 \times 10^{-11}$ |
| 2.0 | $1.72 \times 10^{-11}$ |
| 2.5 | $2.34 \times 10^{-11}$ |
| 3.0 | $1.66 \times 10^{-11}$ |
| 3.5 | $5.80 \times 10^{-11}$ |

where $\varepsilon_0$ is the vacuum permittivity, $\varepsilon$ is the relative permittivity of the medium surrounding the particle, $r_0$ is the particle radius, and $s$ is the distance between two neighboring particles.

The use of scanning electron microscopy (SEM) imaging was employed to image the size and orientation of the particles of the thermally deposited copper films (Figure 6). In Figure 6, a 3 nm film is shown side by side with a 15 nm film, to show the difference in film thickness and orientation at higher depositions, and the 15 nm films show a heavily textured background as a result of the solid metal buildup. An SEM image of an uncoated glass slide is shown in Supporting Figure S2. To analyze the effectiveness of the data obtained using eq 1, in Table 1, we employed the use of the following equation to determine the capacitance of the particles in line with what had been employed by Moskowitz et al.,[15,16] where $d$ represents the diameter of the spherical particle.

$$C = 2\pi\varepsilon_0\varepsilon d \tag{3}$$

It was determined that for the 3 nm film, the average size of the particles was found to be ∼80 nm in diameter, resulting in an average capacitance of about $2.23 \times 10^{-16}$ F for an individual nanoparticle. Based on the spacing shown in the SEM image, it was then determined that there were around 42 individual nanoparticles per 4 $\mu$m distance, resulting in ∼1,05,000 particles per 1 cm distance, the same distance between the two applied electrodes. This would result in an average capacitance of $2.34 \times 10^{-11}$ F for the section of the film in question, which is markedly close to the values that were derived via eq 1, as noted in Table 1.

**3.2. Plasmonic Current and Properties of Copper Nanoparticle Films.** The literature has shown that plasmonic copper films can enhance the emissive properties of fluorophores in the near-field, amplifying their emission while simultaneously shortening their excited-state lifetimes.[19,20,22−24] This process is known as metal-enhanced fluorescence (MEF) and has been observed and reported by several laboratories. The recent literature by our group on fluorophore-induced plasmonic current has noted that there is an inverse relationship between FIPC and MEF,[19,20,22−24] such that a system that would normally produce enhanced MEF emission will produce FIPC under the correct conditions but at the expense of the other. To analyze this relationship for this series of copper films, we initially tested several fluorophores and excitation sources with these copper films. From these initial tests, we found that fluorescein had a dramatic FIPC/MEF response to excitation at 473 nm and was subsequently chosen for study.

Initially, the copper films were placed on the sample stage and treated with 200 $\mu$L of 5 $\mu$M fluorescein. The films and


https://doi.org/10.1021/acsomega.4c02751
ACS Omega 2024, 9, 25181−25188

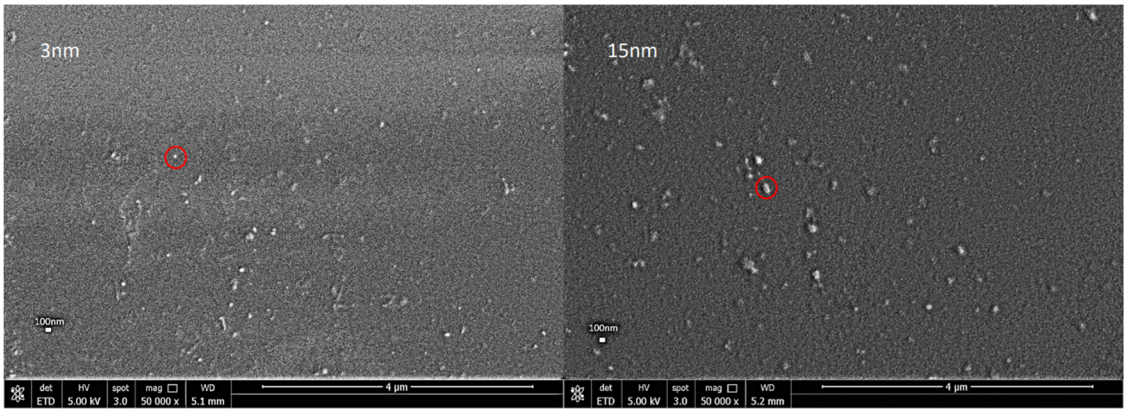


**Figure 6.** SEM images showing two thermally deposited Cu films, 3 nm (left) and 15 nm (right). What can be noted is that as the deposition total increases, the diameter of the individual particles increases and the spacing between them decreases, and in the 15 nm film, the negative space appears to take on more of a textured appearance, suggesting a monolayer continuous deposition of the Cu metal.

fluorophore solution were then connected in series to a Keithley 6487 picoammeter via copper electrodes, and then, a small bias current of 0.005 V was applied, dictating the anode and cathode. The sample was then excited via a 473 nm solid-state laser (Quvl473-20 Laser Mate) and the laser excitation was manually gated 10 times to collect the modulus of the current change both before and after excitation. The emission spectra were subsequently collected via a fiber optic cable spectrophotometer (ocean optics) and are subsequently shown in Figure 4. The electrodes were then removed, and the sample was excited again to now collect the MEF emission from the sample, which was then overlaid with the FIPC emission (Figure 4). We can see that the overall emission of fluorescein is very high for both MEF and FIPC emissions, suggesting that there is a significant amount of far-field fluorescence emission occurring, i.e., uncoupled fluorescence. We can also note that the FIPC emission is consistently lower (weaker) than the MEF emission, and the disparity between the two correlates with the magnitude of the FIPC current we detected through the picoammeter, Table 2. As FIPC conditions become more

**Table 2. Percentage that the MEF Emission Intensity of Fluorescein Was Greater than That for the Intensity When FIPC Was Measured at 515 nm**

| film thickness (nm) | % MEF intensity over PC |
|---|---|
| 1.5 | 5.57 |
| 2.0 | 8.38 |
| 2.5 | 11.10 |
| 3.0 | 6.14 |
| 3.5 | 6.78 |

favorable, in this case, on the 2.5 nm copper film, a larger portion of energy that would be emitted through the fluorescence pathway is instead channeled through the film as plasmonic current.[15−18,24] For all of these experiments, the laser power was held constant.

A concentration series experiment was also undertaken using fluorescein concentrations of 5, 10, 25, 50, and 100 $\mu$M and the experiment was performed in the same manner as the previous literature[24] (Figure 7). We can see that the 2.5 nm films again showed the highest FIPC responses for all fluorophore concentrations, and there is a clear relationship between increasing fluorophore concentration and the FIPC response generated. What is interesting here is that as the peak

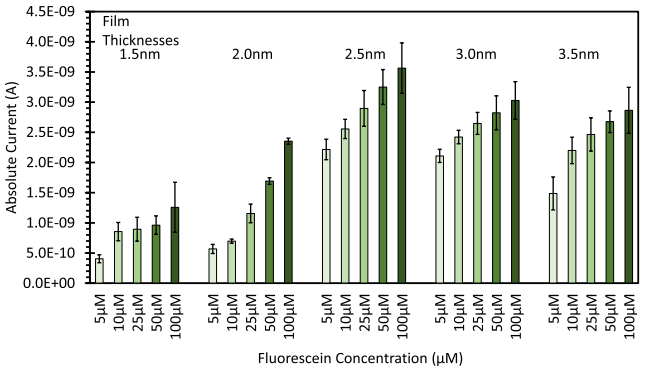


**Figure 7.** Fluorophore-induced plasmonic current (FIPC) responses from various concentrations of fluorescein (5−100 $\mu$M) after their excitation with a 473 nm laser on Cu Films of thickness of 1.5−3.5 nm. These values are calculated from the modulus between the current directly before excitation and subsequently directly after. Each data points are $n$ = 30, i.e., trials of 10 data points in triplicate. A laser power of 10 mW was used.

FIPC response is seen for 2.5 nm Cu, it decreases slightly at larger thicknesses before reaching 4 nm where the film has been shown to be continuous (mirror-like) and less effective. This finding differs from what was seen in the previous literature with regard to FIPC on aluminum films, which were shown to increase in response with increased thickness until the films became continuous.[24] Future work relating to the combination of these two metals will be undertaken to try to understand the relationship between the metals and their ability to produce this FIPC response.

**3.3. Light Polarization and Its Effects on Plasmonic Current Generation.** The recent literature has shown that there is a relationship between the orientation of the polarized excitation light (**S** or **P**) and the magnitude of the generated plasmonic current.[15,24] The literature denotes that the use of polarized light is able to selectively excite the fluorophores such that the mirror dipole created in the film can either result in plasmonic current or result in a scenario where the dipoles cancel each other out and no FIPC is observed. Similarly here, a half-wave plate was used to modify the excitation light, which fall incident 45° to the surface of the film, where the excitation responses are noted from both **P** and **S** orientations; the results are shown in Figure 8. We observed that **P**-polarized light, as expected, was found to produce around 2−2.5× the FIPC


https://doi.org/10.1021/acsomega.4c02751
ACS Omega 2024, 9, 25181−25188

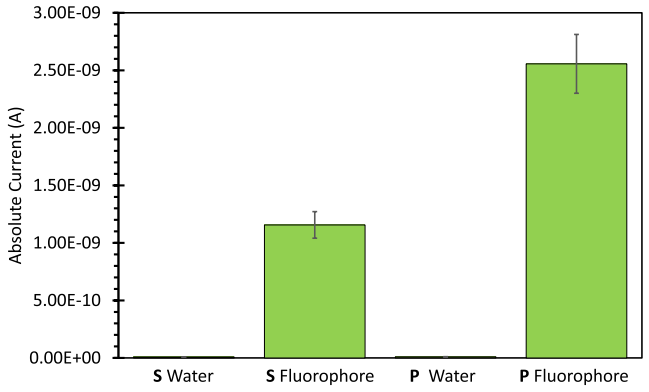


**Figure 8.** Polarization dependence (**S** or **P**) on the magnitude of the fluorophore-induced plasmonic current response (FIPC).

response as compared to the **S**-oriented light, consistent with FIPC-polarized results observed for other metals.[24]

**3.4. Solution Conductance and Its Effect on Plasmonic Current Generation.** It is prudent to question whether the conductance of any solution is additionally playing a role in the magnitude of the induced plasmonic current. To study this, we designed an experiment using 5 $\mu$M solutions of fluorescein, spiked with aqueous solutions of various sulfates (sodium sulfate, magnesium sulfate, and zinc sulfate), and controlling the changes in pH determined their respective absorbance spectra, Supporting Figure S3, and fluorescence spectra $\varepsilon_x$ = 473 nm, Supporting Figure S4, for concentrations of solutes ranging from 1 to 100 $\mu$M. The resistance values across a 2 mm length were determined, Table 3, and the

**Table 3. Resistance and Conductance Values of Various 5 $\mu$M Fluorescein Solutions Spiked with Aqueous Ions**[a]

| | resistance (Ω) | conductance (S) |
|---|---|---|
| 5 $\mu$M fluorescein | $9.92 \times 10^5$ | $1.01 \times 10^{-6}$ |
| 5 $\mu$M fluorescein + 1 $\mu$M Na | $7.41 \times 10^5$ | $1.35 \times 10^{-6}$ |
| 5 $\mu$M fluorescein + 10 $\mu$M Na | $6.30 \times 10^5$ | $1.59 \times 10^{-6}$ |
| 5 $\mu$M fluorescein + 100 $\mu$M Na | $5.87 \times 10^5$ | $1.70 \times 10^{-6}$ |
| 5 $\mu$M fluorescein + 1000 $\mu$M Na | $5.51 \times 10^5$ | $1.81 \times 10^{-6}$ |
| 5 $\mu$M fluorescein + 1 $\mu$M Mg | $7.17 \times 10^5$ | $1.39 \times 10^{-6}$ |
| 5 $\mu$M fluorescein + 10 $\mu$M Mg | $6.72 \times 10^5$ | $1.49 \times 10^{-6}$ |
| 5 $\mu$M fluorescein + 100 $\mu$M Mg | $6.58 \times 10^5$ | $1.52 \times 10^{-6}$ |
| 5 $\mu$M fluorescein + 1000 $\mu$M Mg | $5.38 \times 10^5$ | $1.86 \times 10^{-6}$ |
| 5 $\mu$M fluorescein + 1 $\mu$M Zn | $9.26 \times 10^5$ | $1.08 \times 10^{-6}$ |
| 5 $\mu$M fluorescein + 10 $\mu$M Zn | $7.62 \times 10^5$ | $1.31 \times 10^{-6}$ |
| 5 $\mu$M fluorescein + 100 $\mu$M Zn | $6.56 \times 10^5$ | $1.52 \times 10^{-6}$ |
| 5 $\mu$M fluorescein + 1000 $\mu$M Zn | $5.32 \times 10^5$ | $1.88 \times 10^{-6}$ |
| DI $H_2O$ | $1.67 \times 10^6$ | $5.99 \times 10^{-7}$ |

[a]Resistance measured over a 2 mm distance in a 2.5 mL volume of solution via a FLUKE 179 True RMS Multimeter. Metal ions were all sulfates ($Na_2SO_4$, $ZnSO_4$, and $MgSO_4$).

conductance was calculated. What can be noted from these findings is that for both zinc- and magnesium-doped solutions, there was a decrease in overall fluorescence at the highest concentrations of doped ions, while for the sodium salt, it remained appropriately constant throughout. It was also noted that for all ion solutions, the conductance of the solutions increased as the concentrations of the doped ions increased. After gathering these initial data, these solutions were then used in a plasmonic current generation experiment on a 3 nm Cu film. The solutions were excited via a 473 nm solid-state laser at a fixed power of 24 mW. The results from this experiment are shown in Figure 9. We can see that as

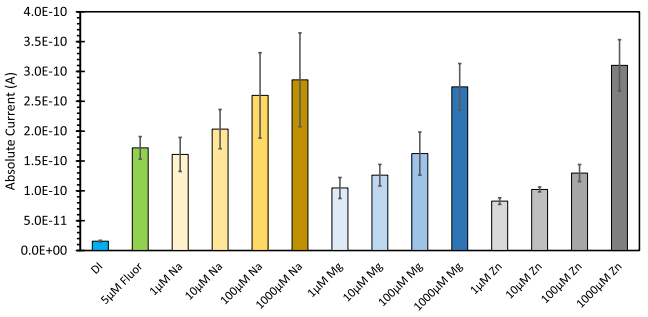


**Figure 9.** FIPC response for 5 $\mu$M fluorescein with various aqueous ions added. The metal ions were all sulfates ($Na_2SO_4$, $ZnSO_4$, and $MgSO_4$).

compared to the control sample of undoped 5 $\mu$M fluorescein, there was a marked increase in the plasmonic current response for the 1000 $\mu$M-doped solutions. There was also a marked increase in each of the specific ion concentration series, with increasing responses for each increase in concentration; however, some of the lower range-doped concentrations were found to be lower than the control of the undoped 5 $\mu$M fluorescein. It is thought that these higher conductance solutions have a higher baseline current when exposed to the bias current applied to the FIPC experiment. This higher baseline current can be seen as a method for signal enhancement if there is a considerable difference between the controls and the fluorophore solutions. Figure 10 shows

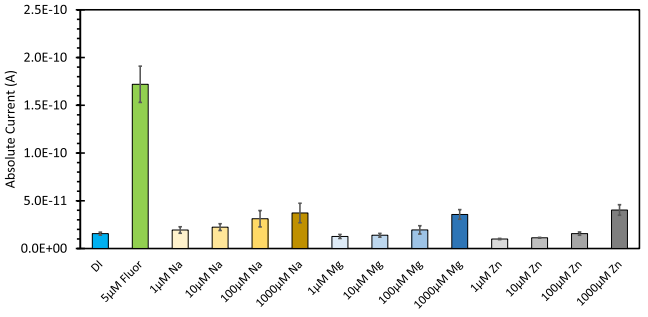


**Figure 10.** FIPC response for 5 $\mu$M fluorescein vs various aqueous solutions of analyte. The metal ions were all sulfates ($Na_2SO_4$, $ZnSO_4$, and $MgSO_4$).

the current of the aqueous metal ions alone without the fluorophore present, and it can be noted that the current change upon excitation increases with the salt concentration for all of the metal species present. These findings show that the conductance of the solution is vital to the generation of plasmonic current and must be controlled, when possible, but also that the introduction of ions may also be used to boost the "signal strength" of fluorophore solutions. This finding could well lead to the addition of inert ions being doped into the system to increase the sensitivity of the responses or to facilitate the usage of a different current detection device at another magnitude of current generation. Finally, we studied the influence of the magnitude of the FIPC as a function of temperature, Supporting Figure S5. As expected, warmer solutions, which have a higher solution conductance, increase


https://doi.org/10.1021/acsomega.4c02751
ACS Omega 2024, 9, 25181−25188

the induced current values, consistent with reports for other metals.[16]

**3.5. Fluorophore Absorption and Its Effect on Plasmonic Current Generation.** To further reinforce a previous notion that the absorption of the fluorophore and its subsequent transfer of excited-state energy to the film are the cause for our generated plasmonic current,[16] a further control experiment was undertaken. A solution of 100 $\mu$M fluorescein was placed onto a 3 nm Cu film, and plasmonic current experiments similar to what was described previously were performed. The notable difference for these experiments was that the excitation sources were changed between four different excitation sources, namely, 266, 473, 532, and 635 nm. The power was regulated via a neutral density filter, and the responses for powers of 2, 4, 6, 8, and 10 mW are shown in Figure 11. We can see that the peak plasmonic current

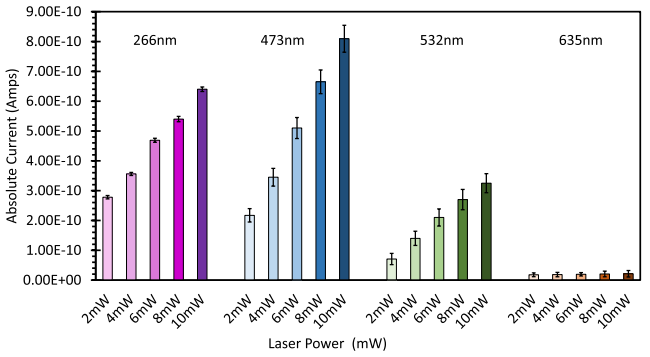


**Figure 11.** Responses of a 100 $\mu$M solution of fluorescein on a 3 nm Cu film, excited at four different wavelengths, 266 nm (far left), 473 nm (center left), 532 nm (center right), and 635 nm (far right) at various power settings. Power was controlled via a neutral density filter, and power readings were collected via a 200−1100 nm digital hand-held Thor laboratories optical power meter.

response can be seen to align itself with the approximate absorbance spectra of fluorescein, shown in Supporting Figure S3, such that the higher the absorbance of fluorescein, the higher the response of the current. The modulation of the power in the system also confirms that as we increase the amount of light absorbed by the sample, the response of the system subsequently increases for all wavelengths, even at 635 nm, which is difficult to see on this scale as there is very little overlap between fluorescein absorption and red light.

## 4. CONCLUSIONS

We have shown in this study that copper nanoparticle films are suitable substrates for the generation of plasmonic current. It has been shown that there is an optimal film thickness of FIPC generation. A film that is too thin will result in limited coupling by the fluorophores, and a film that is too thick will lose the signal generated to background noise and ohmic loss, i.e., above 4 nm thickness for Cu films. The particles must be isolated from each other such that the individual nanoparticles charge and discharge, leading to electron hopping. These films have been characterized by their absorbance and response to voltage sweeps. The capacitance of these films has been calculated and shown to be consistent with similar films of its type. The conductance of the solution and temperature of the films influence the response of the plasmonic current generation and can be tuned to better design detection schemes. A MEF vs FIPC analysis shows that the copper films operate best at ∼2.5 nm thickness, and the concentration dependence on FIPC generation supports this finding. These films have the potential to be a robust method of fluorescence detection without the need for traditional optical detection equipment.

## ■ ASSOCIATED CONTENT

### Supporting Information

The Supporting Information is available free of charge at https://pubs.acs.org/doi/10.1021/acsomega.4c02751.

Absorbance spectra for 1−15 nm cu films, SEM imaging of control slides prior to copper deposition, absorbance and fluorescence data for fluorescein with added aqueous ions, temperature control data for FIPC measurements, and structure of fluorescein (PDF)

## ■ AUTHOR INFORMATION


### Corresponding Author

**Chris D. Geddes** − *Institute of Fluorescence, and Department of Chemistry and Biochemistry, University of Maryland, Baltimore County, Baltimore, Maryland 21202, United States*; Phone: 1 410 706-3149; Email: Geddes@umbc.edu

### Authors

**Daniel R. Pierce** − *Institute of Fluorescence, and Department of Chemistry and Biochemistry, University of Maryland, Baltimore County, Baltimore, Maryland 21202, United States*; orcid.org/0000-0003-0382-1966

**Lahari Saha** − *Institute of Fluorescence, and Department of Chemistry and Biochemistry, University of Maryland, Baltimore County, Baltimore, Maryland 21202, United States*

Complete contact information is available at: https://pubs.acs.org/10.1021/acsomega.4c02751


### Notes

The authors declare no competing financial interest.

## ■ ACKNOWLEDGMENTS

The authors acknowledge salary support to C. D. Geddes from UMBC and support to Daniel. R. Pierce from the Chemistry-Biology Interface program (CBI) grant #5T32GM066706. The authors also acknowledge the GRISE program grant #1T32GM144876-01 for salary support for Lahari Saha.

## ■ ACRONYMS AND SYMBOLS

**MEF** = metal-enhanced fluorescence
**FIPC** = fluorophore-induced plasmonic current
**MNFs** = metal nanoparticle films

## ■ REFERENCES


(1) Lakowicz, J. R. *Principles of Fluorescence Spectroscopy*; Springer: New York, 2006.

(2) Geddes, C. D.; Aslan, K. *Metal-Enhanced Fluorescence: Progress Towards a Unified Plasmon-Fluorophore Description*; John Wiley & Sons: New Jersey, 2010.

(3) Eustis, S.; El-Sayed, M. Aspect Ratio Dependence of the Enhanced Fluorescence Intensity of Gold Nanorods: Experimental and Simulation Study. *J. Phys. Chem. B* **2005**, *109*, 16350−16356.

(4) Pelton, M.; Bryant, G. W. *Introduction to Metal-Nanoparticle Plasmonics*; John Wiley & Sons: Hoboken, NJ, 2013.

(5) Li, J.; Krasavin, A. V.; Webster, L.; Segovia, P.; Zayats, A. V.; Richards, D. Spectral variation of Fluorescence Lifetime Near Single Metal Nanoparticles. *Sci. Rep.* **2016**, *6*, No. 21349.
(6) Weitz, D. A.; Gersten, S.; Garoff, C. D.; Hanson, T. J.; Gramila, J. I. Fluorescent Lifetimes of Molecules on Silver-Island Films. *Opt. Lett.* **1982**, *7*, 89−91.
(7) Gupta, R.; Dyer, M. J.; Weimer, W. A. Preparation and Characterization of Surface Plasmon Resonance Tunable Gold and Silver Films. *J. Appl. Phys.* **2002**, *92*, 5264−5271.
(8) Homola, J. *Surface Plasmon Resonance based Sensors*; Springer: Berlin, Germany, 2006.
(9) Wei, W.; Zhang, X.; Ren, X. Plasmonic Circular Resonators for Refractive Index Sensors and Filters. *Nanoscale Res. Lett.* **2015**, *10*, No. 211, DOI: 10.1186/s11671-015-0913-4.
(10) Skoog, D. A.; West, D. M. *Principles of Instrumental Analysis*; Holt, Rinehart and Winston: New York, 2010.
(11) Jeanmaire, D. L.; Van Duyne, R. P. Surface Raman Spectroelectrochemistry Part I. Heterocyclic, Aromatic, and Aliphatic Amines Adsorbed on the Anodized Silver Electrode. *J. Electroanal. Chem.* **1977**, *84*, 1−20.
(12) Le Ru, E. C.; Blackie, E.; Meyer, M.; Etchegoin, P. G. Surface Enhanced Raman Scattering Enhancement Factors: A Comprehensive Study. *J. Phys. Chem. C* **2007**, *111*, 13794−13803.
(13) Kawata, S.; Inouye, Y.; Verma, P. Plamsonic for Near Field Nano Imaging and Super Lensing. *Nat. Photonics* **2009**, *3*, 388−394.
(14) Gotte, J. Principles of Nano-Optics. *Contemp. Phys.* **2013**, *54*, 123−124, DOI: 10.1080/00107514.2013.800150.
(15) Moskowitz, J.; Geddes, C. D. Plasmonic Electricity: Fluorophore-Induced Plasmonic Current. *J. Phys. Chem. C* **2019**, *123*, 27770−27777.
(16) Moskowitz, J.; Sindi, R.; Geddes, C. D. Plasmonic Electricity II: The Effect of Particle Size, Solvent Permittivity, Applied Voltage, and Temperature on Fluorophore-Induced Plasmonic Current. *J. Phys. Chem. C* **2020**, *124*, 5780−5788.
(17) Knoblauch, R.; Moskowitz, J.; Hawkins, E.; Geddes, C. D. Fluorophore-Induced Plasmonic Current: Generation-Based Detection of Singlet Oxygen. *ACS Sens.* **2020**, *5*, 1223−1229.
(18) Moskowitz, J.; Geddes, C. D. The Inverse Relationship between Metal-Enhanced Fluorescence and Fluorophore-Induced Plasmonic Current. *J. Phys. Chem. Lett.* **2020**, *11*, 8145−8151.
(19) Golberg, K.; Elbaz, A.; Zhang, Y.; Dragan, A. I.; Marks, R.; Geddes, C. D. Mixed-Metal Substrates for Applications in Metal-Enhanced Fluorescence. *J. Mater. Chem.* **2011**, *21*, 6179−6185.
(20) Previte, M. J. R.; Geddes, C. D. Microwave-Triggered Chemiluminescence with Planar Geometrical Aluminum Substrates: Theory, Simulation and Experiment. *J. Fluoresc.* **2007**, *17*, 279−287.
(21) Aslan, K.; Malyn, S. N.; Zhang, Y.; Geddes, C. D. Conversion of Just-Continuous Metallic Films to Large Particulate Substrates for Metal-Enhanced Fluorescence. *J. Appl. Phys.* **2008**, *103*, No. 084307.
(22) Chowdhury, M. H.; Ray, K.; Gray, S. K.; Pond, J.; Lakowicz, J. R. Aluminum Nanoparticles as Substrates For Metal-Enhanced Fluorescence in the Ultraviolet for The Label-Free detection of Biomolecules. *Anal. Chem.* **2009**, *81*, 1397−1403.
(23) Sultangaziyev, A.; Akhmetova, A.; Kunushpayeva, Z.; Rapikov, A.; Filchakova, O.; Bukasov, R. Aluminum Foil as a Substrate for Metal Enhanced Fluorescence of Bacteria Labelled with Quantum Dots, Shows Very Large Enhancement and High Contrast. *Sens. Bio-Sens. Res.* **2020**, *28*, No. 100332.
(24) Pierce, D. R.; Bobbin, M.; Geddes, C. D. Fluorophore-induced plasmonic current generation from aluminum nanoparticle films. *J. Phys. Chem. C* **2023**, *127* (2), 1126−1134.


https://doi.org/10.1021/acsomega.4c02751
*ACS Omega* 2024, 9, 25181−25188